Bias correction demonstration in two of the Indian Himalayan river basins

A. P. Dimri

ABSTRACT

There is imperative need of robust basin-scale data for climate impact studies over the topographically varying and landuse heterogenous river basins in the Indian Himalayan Region (IHR). Even finer resolution regional climate models' (RCMs) information is elusive for these purposes. Based on available model fields and corresponding *in-situ* observed fields, bias correction for precipitation over Upper Ganga River Basin (UGRB) and temperature over Satluj River Basin (SRB) is demonstrated. These chosen river basins are in central and western Himalayas, respectively. Model precipitation (temperature) field from RegCM4.7 (REMO) and corresponding observed precipitation (temperature) field from nine (eight) stations of UGRB (SRB) are considered. Empirical quantile mapping (inverse function method) method is used. It is seen that each model has a distinct systematic bias relating to both precipitation and temperature means with respect to their corresponding observed means. Applying bias correction methods to the model fields resulted in reducing these mean biases and other errors. These findings illustrate handling and improving the model fields for hydrology, glaciology studies, etc.

Key words | bias correction, Himalayan River Basin, Indian Himalayan Region, precipitation, temperature

HIGHLIGHTS

- Bias correction using empirical quantile mapping (inverse function method) is employed on both precipitation and temperature model.
- Applying bias correction methods to the model fields resulted in reducing the mean biases and other errors.
- These findings illustrate handling and improving the model fields for hydrologist, glaciologist, etc.

A. P. Dimri
School of Environmental Sciences,
Jawaharlal Nehru University,
New Delhi,
India
110067
E-mail: *apdimri@hotmail.com*

doi: 10.2166/wcc.2020.119

GRAPHICAL ABSTRACT

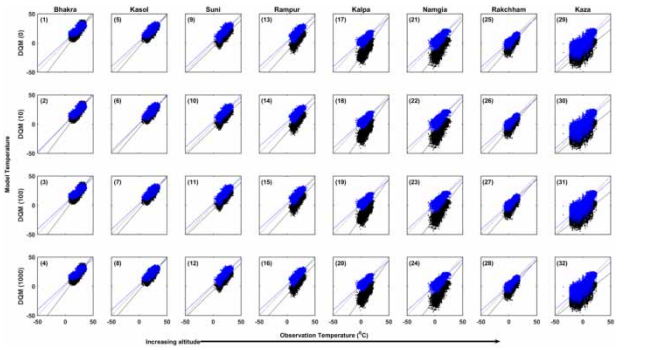

INTRODUCTION

The Himalayas is the source of many north Indian rivers, namely, Indus, Satluj, Ganges, Brahmaputra, etc. These rivers support millions of downstream populations which are dependent on agriculture and pasture usages, water resources for domestic usages, hydro-electric dams, industries, etc. These rivers are mainly fed by monsoonal precipitation and spring snowmelt from high elevation glaciers and the cryosphere (Eriksson *et al.* 2009; Bookhagen & Burbank 2010; Palazzi *et al.* 2013; Norris *et al.* 2015, 2017; Bannister *et al.* 2019). Most of the rivers originating from the western Himalayas are mainly fed by the Indian winter monsoon (Dimri *et al.* 2016) embedding western disturbances (Dimri *et al.* 2015); and rivers originating from the central and eastern Himalayas are mainly fed by the Indian summer monsoon (Maharana & Dimri 2019).

Most of the Indian Himalayan river basins have variable topography and heterogeneous landuse/landcover. These basins are data sparse as well. Usage of dynamical or statistical or statistical–dynamical downscaled model outputs at finer resolutions are greatly needed for climate impact studies for hydrological, glaciological and water resources (Akhtar *et al.* 2008; Narula & Gosain 2013; Sanjay *et al.* 2017). However, over river basins having complex topography and landuse, these finer resolution model inputs are still not sufficient as they have systematic biases due either to model physics or parameterization. Improving these model fields further by reducing these biases/errors is important. Choudhary & Dimri (2019) have discussed various bias correction methods, their strengths and weaknesses. Bannister *et al.* (2019) have carried out bias correction in two of the western Himalayan river basins using *in-situ* observations and made an assessment of precipitation extremes. These regions have strong precipitation and temperature gradients which are difficult to produce in a model environment and, at times, are elusive as well. Hence, representation or usage of these model fields directly for impact studies is not suitable or ideal. There are some studies on precipitation and temperature bias corrections over complex topographical mountainous regions (Christensen *et al.* 2008; Piani *et al.* 2010; Bordoy & Burlando 2013; Shrestha *et al.* 2017). Yet, these studies fall short in providing comprehension regarding the Indian Himalayan river basins.

In the present paper, we have shown precipitation bias correction over the Upper Ganga River Basin (UGRB), in central Himalayas, and Satluj River Bain (SRB), in western Himalayas.

STUDY REGIONS

The study is conducted over two important river basins: (1) Upper Ganga River Basin (UGRB) – a sub-basin of the Ganga river system in central Himalayas (Figures 1(a) and 2) Satluj River Basin (SRB) – in western Himalayas (Figure 1(b)).

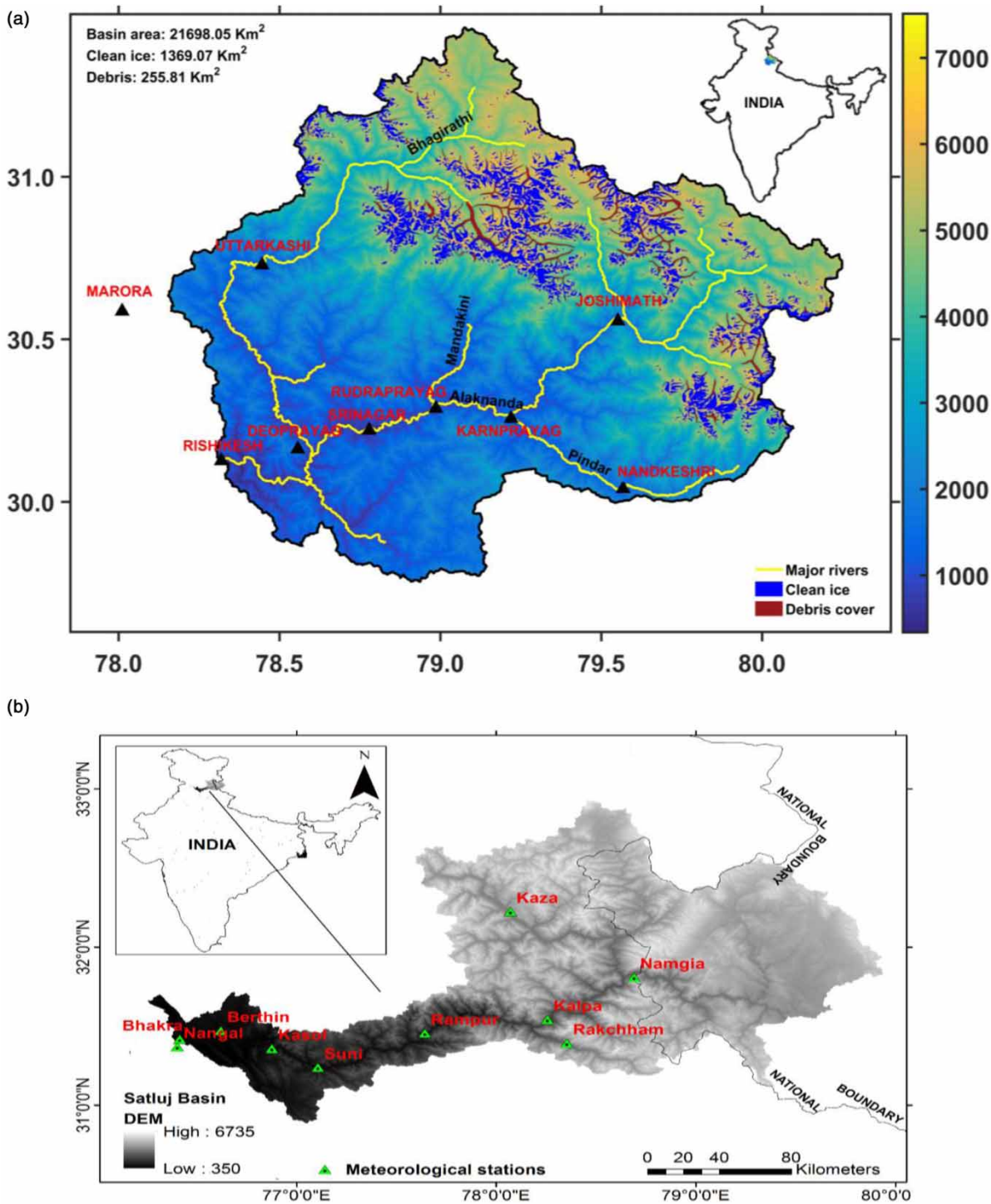

Figure 1 | Study area: (a) Upper Ganga River Basin (UGRB) with nine precipitation *in-situ* observation stations (Rishikesh, Devprayag, Srinagar, Rudraprayag, Karanprayag, Marora, Uttarkashi, Nandkeshri and Joshimath) scattered over the UGRB in central Himalayas. The elevation is shown in the background with Shuttle Radar Topographic Mission (SRTM) digital elevation model (DEM) with 90 m resolution. (b) Sutlej River Basin (SRB) with eight temperature *in-situ* observation stations (Bhakra, Kasol, Suni, Rampur, Kalpa, Namgia, Rakchham and Kaza) scattered over the SRB in western Himalayas. The topography is variable from 350 m to as high as 6,735 m. It is shown with 90 m resolution DEM from SRTM. Triangles represent the different observation stations used in the study.

Upper Ganga River Basin (UGRB)

The Ganga is the longest river of India and ranks among the world's top 20 rivers by amount of water discharge. The Ganga River Basin covers an area of ~981,371 km^2 shared by India, Nepal, China and Bangladesh. It originates at the confluence of the Bhagirathi and Alaknanda rivers, at Devprayag in Tehri Garhwal district of Uttarakhand State of India – within the mountainous region of the lower Himalayas. The river travels a distance of ~2,520 km before merging with the Bay of Bengal. Throughout its length, a number of tributaries join it. The principal tributaries joining are the Yamuna, Ramganga, Ghaghra, Gandak, Kosi, Mahananda and Son. The Ganga River is divided into three distinct zones, i.e., Upper Ganga Basin, Middle Ganga Basin and Lower Ganga Basin.

The focus of the present study is on the UGRB – which is delineated and shown in Figure 1(a) using the 90 m SRTM digital elevation map. The total area of the UGRB is ~21,698.05 km^2. The basin has a significant amount of glacier cover including debris cover glaciers. The elevation in the UGRB ranges from 7,500 m in the Himalayan mountain region to 100 m in the lower plains. Around 60% of the basin is occupied by agriculture (main crop types include wheat, maize, rice, sugarcane, bajra and potato), while 20% is covered by forests, mostly in the upper mountainous regions, and approximately 2% of the mountain peaks are permanently snow covered. The annual average rainfall in the UGRB ranges between 550 and 2,500 mm (Bharati & Jayakody 2010), and a major part of the rain is due to the Indian summer monsoon.

Long-term and good quality daily *in-situ* precipitation observations at nine stations, as shown in Figure 1(a) and Table 1, are considered.

Satluj River Basin (SRB)

The SRB, one of the main tributaries of the Indus river system, is also considered for the study. The river originates from the lakes of Mansarover and Rakastal in the Tibetan Plateau at an elevation of about 4,572 m. The Indian part of the SRB covers an area of ~22,305 km^2 (Figure 1(b). The topography varies from 350 m to as high as 6,735 m, and is shown with the 90 m resolution DEM from Shuttle Radar Topographic Mission (SRTM). About 57% of the basin area lies between 3,600 and 5,400 m altitude; only a small fraction of the area is above 6,000 m. The topographical setting and the abundant availability of water provide huge hydropower generation potential, and hence several hydropower schemes exist and/or are planned on this river. Bhakra Dam, the oldest dam in India, is situated on this river, in the foothills of the Himalayas. Due to the wide range of altitudes and precipitation patterns, a diverse climate is experienced in the basin. The lower part of the basin has tropical and warm temperate climate, whereas the middle part has a cold temperate climate. In the upper part, the climate is very cold and in the uppermost part, which is a perpetually frozen area (permafrost), the climate

Table 1 | Details of *in-situ* precipitation observations used in the study of UGRB

S. No.	Station name	Long. (deg)	Lat. (deg)	Elevation (m)	Date length	Total years
1	Rishikesh	78 18 14	30 06 03	327	1975–2005	31 years
2	Devprayag	78 34 02	30 09 43	452	1975–2005	31 years
3	Srinagar	78 46 46	30 13 13	530	1990–2005	16 years
4	Rudraprayag	78 59 10	30 17 15	614	1975–1987	13 years
5	Karanprayag	79 13 11	30 15 22	765	1986–2005	20 years
6	Marora	78 42 05	29 56 10	547	1975–2005	31 years
7	Uttarkashi	78 26 46	30 43 42	1,095	1979–2005	27 years
8	Nandkeshri	79 29 48	30 04 42	1,260	1995–2005	11 years
9	Joshimath	79 33 07	30 33 60	1,375	1975–2005	31 years

Source: Central Groundwater Commission (CWC) through NIH, Roorkee under NMSHE project.

is similar to that of polar regions. The upper part of the basin mostly receives solid precipitation by the Indian winter monsoon embedding western disturbances, whereas the middle part receives both rain and snow and the lower part of the basin receives only rain. The average annual rainfall in the lower, middle and greater Himalayan basin regions is about 1,300, 700 and 200 mm, respectively (Singh & Kumar 1997).

To demonstrate the bias correction of temperature in this basin, eight *in-situ* observations are used as shown in Figure 1(b) and Table 2.

METHOD: BIAS CORRECTION

The bias corrections are performed on the regional climate model (RCM) outputs. For precipitation field, RegCMver4.7 setup was used under three different land surface characterization schemes, namely, CONTROL, CLM4.5 and SUBGRID BATS (details are provided in the Supplementary material and Table S1). Corresponding model topography over the UGRB is shown in Figure 2. For temperature, CORDEX-REMO model outputs are chosen. (For model precipitation and temperature fields different RCMs are chosen. Deliberation and discussion on using and picking different models is beyond the scope of this paper and hence not provided. Please refer to Choudhary & Dimri (2019). In addition, there is limitation of the *in-situ* observations, hence over the UGRB precipitation, and over the SRB, temperature fields are considered).

Precipitation bias correction

The precipitation bias correction is performed using nine *in-situ* observations distributed across the UGRB (Figure 1(a) and Table 1). The data range and stations' details are shown in the table. It is imperatively important to mention that precipitation variability over the varying topographic region is always a key issue as complex topographic regions within the model physics and processes thereof are not truly captured (Norris *et al.* 2017; Bannister *et al.* 2019).

Table 2 | Details of *in-situ* temperature observations used in the study of SRB

S.No.	Station name	Long.	Lat.	Elevation (m)	Data length	Total years
1	Bhakra	76.4334°E	31.4112°N	518	1978–2005	28 years
2	Kasol	77.3150°E	32.0100°N	622	1964–2005	42 years
3	Suni	77.1221°E	31.2422°N	655	1970–1998	29 years
4	Rampur	77.6298°E	31.4492°N	976	1978–2005	28 years
5	Kalpa	78.2754°E	31.5377°N	2,439	1984–2005	22 years
6	Namgia	78.6565°E	31.8097°N	2,910	1984–2005	22 years
7	Rakchham	78.3643°E	31.3790°N	3,130	1994–2005	12 years
8	Kaza	78.0710°E	32.2276°N	3,639	1984–2004	21 years

Source: Central Groundwater Commission (CWC) through NIH, Roorkee under NMSHE project.

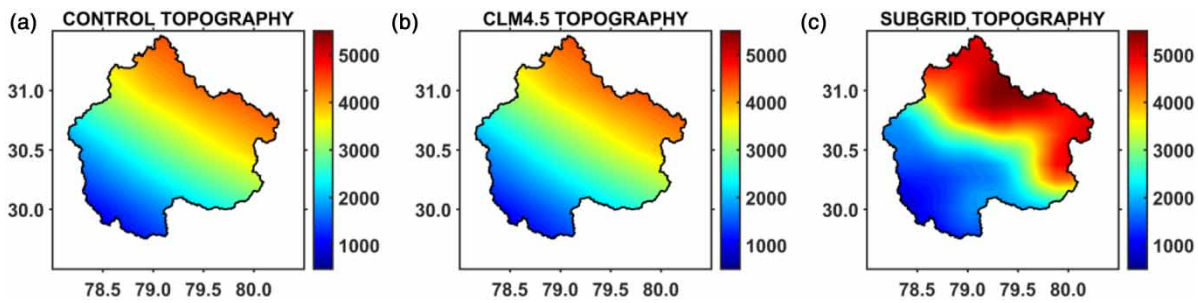

Figure 2 | Model topography of CONTROL, CLM4.5 and SUBGRID scheme within the regional climate model (RegCM ver 4.7) framework over the UGRB.

The bias correction is performed through the empirical quantile mapping method. The wet and dry day threshold for the analysis is kept at 0.1 mm. The tri-cubic function was used to fit the data between each quantile. Bias correction is performed such that the distribution of observed and modelled precipitation matches well:

$$p^{\wedge}_{obs} = F^{-1}_{obs}(F_{mod}(p_{mod}))$$

where F^{-1}_{obs} is inverse CDF of p_{obs}; and F_{mod} is the CDF of p_{mod}. p_{obs} and p_{mod} represents the probability of observation and model precipitation, respectively. The probability of the occurrence of dry days is accounted by using Bernoulli's distribution. The drizzle and dry days' threshold is kept as 0.1 mm.

Temperature bias correction

The temperature bias correction is performed using eight *in-situ* observations distributed across the SRB (Figure 1(b) and Table 2). Distributed quantile mapping on the normal distribution of temperature is used as the temperature is well approximated through the normal distribution. The normal distribution with mean μ and standard deviation σ for the temperature data are approximated as:

$$f_N(x \vee \mu, \sigma) = \frac{1}{\sigma \times \sqrt{2\pi}} \times e^{\frac{-(x-\mu)^2}{2\sigma^2}}$$

The bias correction was performed as the inverse function of the observed temperature over the model temperature as:

$$p^{\wedge}_{obs} = F^{-1}_{obs}(F_{mod}(p_{mod}))$$

where, F^{-1}_{obs} is inverse CDF of p_{obs}; and F_{mod} is the CDF of p_{mod}. p_{obs} and p_{mod} represents the probability of observation and model temperature, respectively.

RESULTS AND DISCUSSION

In the following sections firstly, *precipitation bias correction over UGRB* is demonstrated using RegCMver 4.7 model precipitation field. It is followed by *temperature bias correction over SRB* using REMO model temperature field. (Model fields chosen for bias correction are from different RCMs. Deliberation and discussion on using and picking different model sets is beyond the scope of this paper and hence not provided. In addition, there is limitation of *in-situ* observations, hence over the UGRB precipitation, and over the SRB temperature fields are considered).

Precipitation bias correction over UGRB

Many authors (Ali *et al.* 2015; Li *et al.* 2016; Nepal 2016; Bannister *et al.* 2019) have worked on precipitation bias correction. However, it is important to improve upon and to include the role of model topography and associated physical processes to be captured in bias correction method. Here, precipitation percentage bias (PBIAS) is a measure of estimating the average tendency of the model precipitation field to be larger or smaller than the corresponding *in-situ* precipitation observation. Figure 3 illustrates this precipitation percentage bias at the nine stations in the UGRB. It is clearly seen that at six (three) stations, precipitation percentage bias is positive (negative). It corresponds that at six (three) stations average tendency of model precipitation field is larger (smaller) than the corresponding *in-situ* observation. It is interesting to note that as we move from lower to higher elevation stations, the measure of percentage bias tendency starts decreasing and finally reverses over the highest elevation stations. This corresponds to the role of precipitation forming mechanism and associated physical processes such that, over the lower elevation regions, in the model environment, leads to a drift away of the amount of precipitation from the actual than compared over the higher elevation regions. To further look into the precipitation and associated complexities over the mountainous region, wet periods (days) in logarithmic frequency distribution with bias correction at one of the station, Devprayag, is shown in three model simulations: CONTROL (Figure 4(a)), CLM4.5 (Figure 4(b)) and SUBGRID (Figure 4(c)). It is necessary to mention that in all the three simulation experiments, longer wet spell periods are not well captured.

Still employing bias correction method with corresponding *in-situ* observation at Devprayag, improvement in the wet spell periods, although in lower length, is distinctly

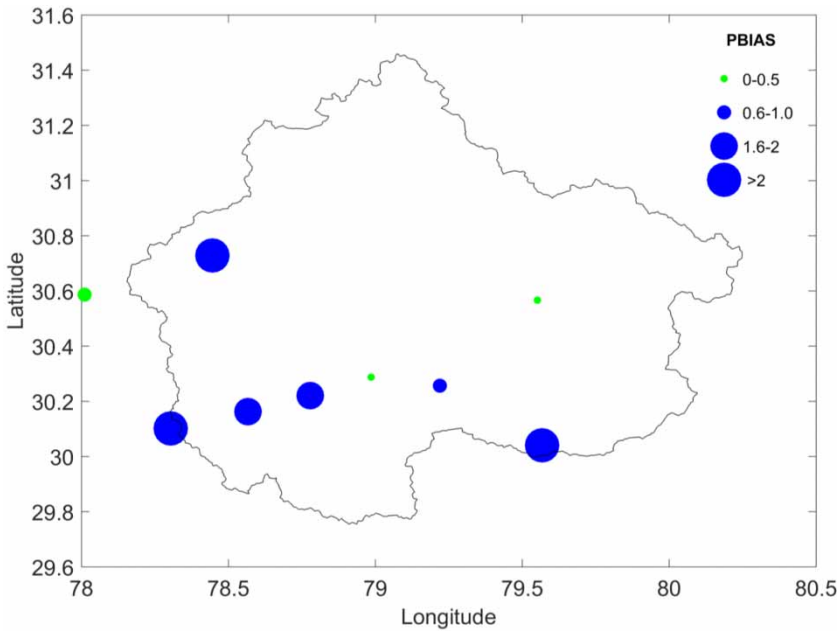

Figure 3 | Percentage bias (PBIAS) of the bias correction of precipitation of the CONTROL model precipitation field with the corresponding *in-situ* observed precipitation field at nine stations (Rishikesh, Devprayag, Srinagar, Rudraprayag, Karanprayag, Marora, Uttarkashi, Nandkeshri and Joshimath) in the UGRB. The positive and negative biases are shown. The size of bubbles corresponds to increase or decrease of bias.

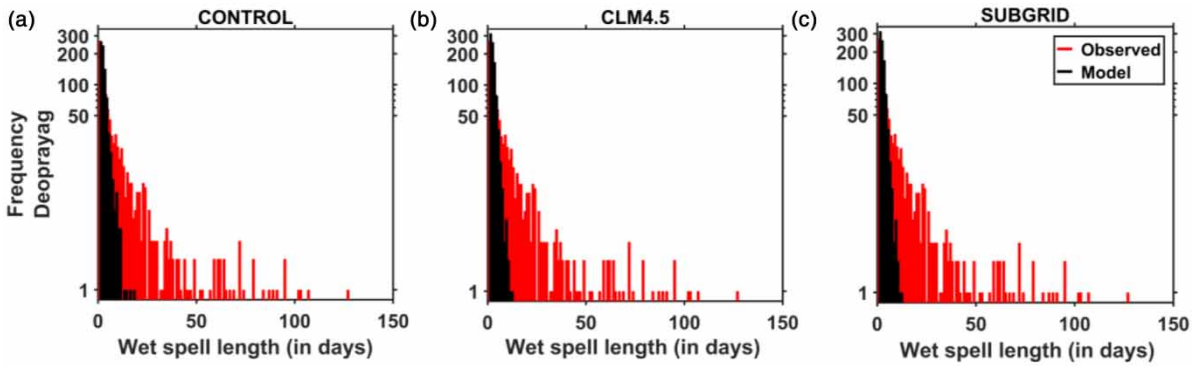

Figure 4 | The frequency of wet spell length at Devprayag station under (a) CONTROL, (b) CLM4.5 and (c) SUBGRID simulations. The black bar represents the bias corrected model wet spell length and bar represents corresponding observed wet spell length. The frequency distribution (y-axis) is in logarithmic scale and the number of continuous rainy days are presented in the x-axis.

seen. Lower wet spell period counts mainly have higher frequencies. To improve upon this further, quantile–quantile (q-q) bias correction method is employed upon the model daily precipitation field from three simulations – CONTROL, CLM4.5 and SUBGRID – using corresponding *in-situ* daily precipitation at nine stations in the UGRB and presented in Figure 5. Comparison on scatter distribution of model and *in-situ* precipitation fields shows higher deviation for higher intensity precipitation events. Comparison on q-q scale of non-bias corrected precipitation distribution shows comparatively better distribution along the slope of distribution. However, q-q scale of bias corrected precipitation fields shows best distribution along the slope of the distribution. This improved bias corrected model precipitation field is important for river basins like the UGRB. q-q distributions in figures illustrate distinct improvement in the model precipitation field after employing bias correction. It is quite clear that over a smaller

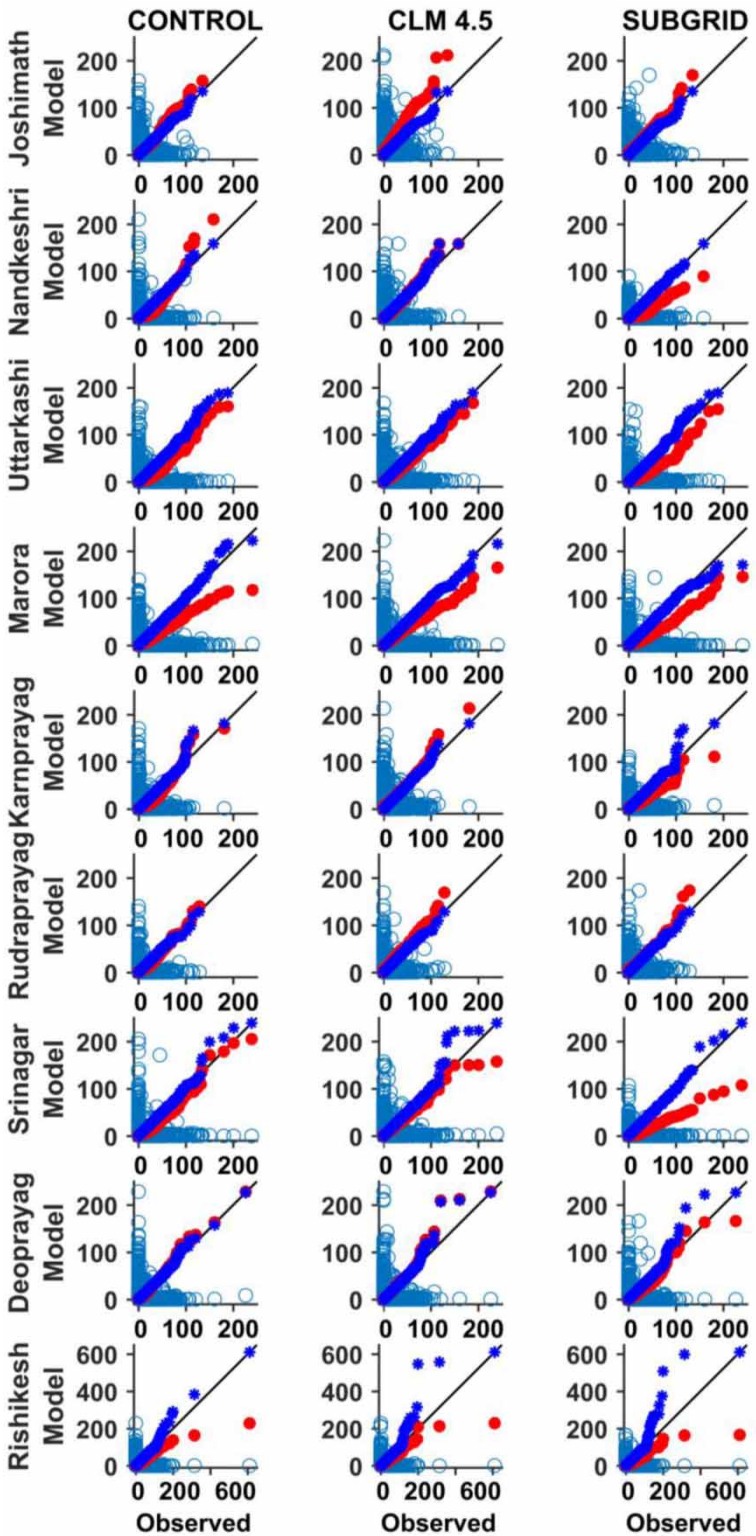

Figure 5 | The q-q (quantile–quantile) distribution of precipitation field at nine stations (Rishikesh, Devprayag, Srinagar, Rudraprayag, Karanprayag, Marora, Uttarkashi, Nandkeshri and Joshimath) in the UGRB with three model simulations: CONTROL, CLM4.5 and SUBGRID, respectively. Empty circles represent the scatter plot between observed and model precipitation fields. Dark filled circles represent the q-q distribution of non-bias corrected model precipitation field and light filled circles represent the q-q distribution of bias corrected model precipitation field with the corresponding observed temperature field.

river basin such efforts of bias correction will be needed for bias corrected model fields. Non-bias corrected data show that model precipitation fields have lower values than that of the corresponding observed precipitation field, which after employing the bias correction, shows that bias corrected model precipitation fields are closer to observed precipitation fields.

Temperature bias correction over SRB

To demonstrate bias correction on model temperature, fields from REMO models are chosen (not discussed in detail due to brevity being beyond the scope of the paper). Temperature bias correction is carried over the SRB where there is long-term (1961–2005) data at eight stations. Figure 6 shows the probability density function (pdf) of bias corrected model temperature field of REMO with the corresponding observations at eight stations (Bhakra, Kasol, Suni, Rampur, Kalpa, Namgia, Rakchham and Kaza) in the SRB during a historical time period (1961–2005). The figure represents the distribution of *in-situ* observed, model and bias corrected temperature field. All distributions are Gaussian distribution. Almost at all stations (vertically in different numbers of quantile used), distributed quantile mappings (DQMs) follow similar distributions which illustrates that the bias correction method employed is quite good at capturing the distribution of temperature. Pdf distribution at different stations are shown by different peaks and spread indicating the variabilities. Lower range of spread indicates the lesser variability among the temperature values. Also, the low probability of temperature indicates that the temperature has comparatively smoother distribution between its lowest and highest value leading to reduced mean. The flattened pdf at Kaza, which is a high-altitude station, shows lesser mean but higher limited variability between lowest and highest values. On comparison with the observed and model pdf of the temperature field, skewness (mostly towards left) and either decreased or increased mean values are seen. On employing the bias correction method, bias corrected temperature distributions are found closer to the corresponding observations. Table 3 illustrates improvement in

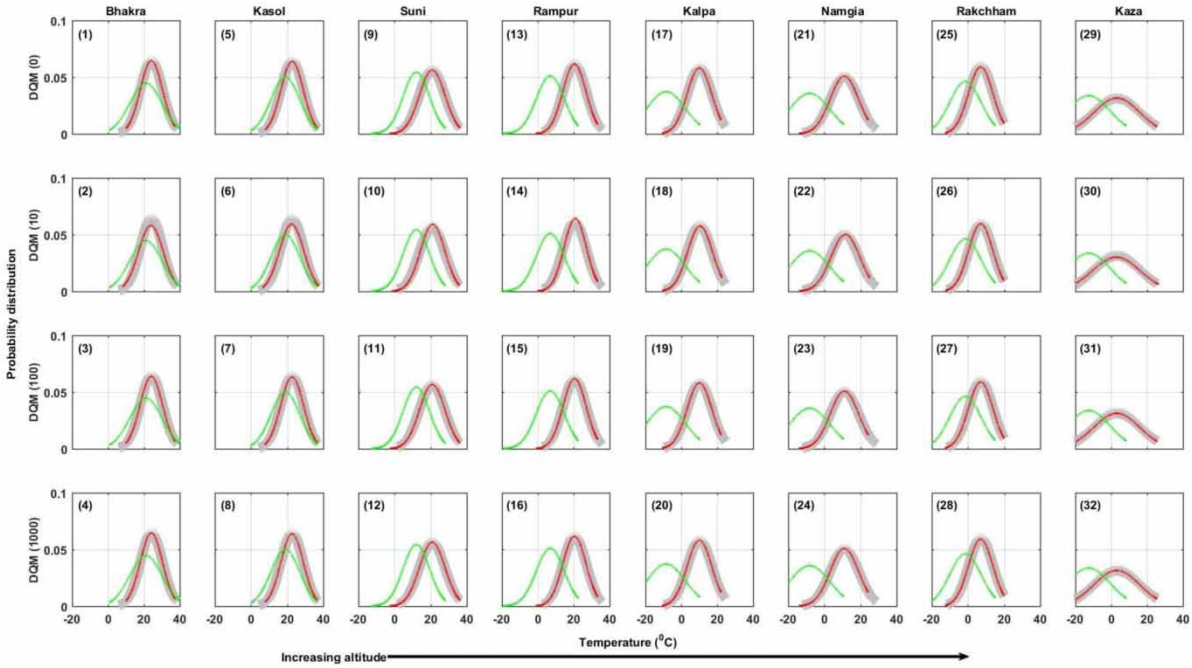

Figure 6 | The probability density function (pdf) of model temperature field, bias corrected temperature field and corresponding observed temperature field at eight stations (Bhakra, Kasol, Suni, Rampur, Kalpa, Namgia, Rakchham and Kaza) in the SRB during a historical time period (1961–2005). The shaded colour represents the distribution of *in-situ* temperature observations, lighter colour represents the distribution of model temperature field and dark colour represents the distribution of bias corrected temperature field. All distributions are Gaussian distribution. DQM stands for distributed quantile mapping and the number within the brackets (0, 10, 100, 1,000) represents the number of quantile used in the particular study to divide data length.

Table 3 | The four statistics mean, mode, skewness and kurtosis from all stations

Stations		Bhakra	Kasol	Suni	Rampur	Kalpa	Namgia	Rakchham	Kaza
Mean	Observation	24.248	22.774	20.803	20.517	10.194	11.135	7.1952	3.2686
	Model	21.16	19.054	12.092	6.974	−8.5172	−8.1399	−1.359	−12.505
	DQM (0)	24.183	22.76	20.881	20.432	10.092	11.052	7.084	3.1626
	DQM (10)	23.929	22.509	21.122	20.882	10.469	11.67	7.1085	2.8406
	DQM (100)	24.17	22.747	20.894	20.495	10.129	11.105	7.0685	3.1014
	DQM (1,000)	24.181	22.757	20.884	20.436	10.094	11.057	7.0849	3.1558
Mode	Observation	28.5	27.2	26.65	26.65	18.25	20.5	15.75	0
	Model	24.427	26.219	19.246	−0.54	−14.498	−17.37	5.789	−17.682
	DQM (0)	26.438	28.36	27.77	14.218	6.2807	4.5873	12.668	−2.3524
	DQM (10)	26.437	28.561	27.705	14.907	6.6134	5.11	12.644	−2.9575
	DQM (100)	26.453	28.407	27.739	14.315	6.3139	4.6391	12.66	−2.4745
	DQM (1,000)	26.439	28.364	27.767	14.222	6.2823	4.5938	12.668	−2.3655
Skewness	Observation	−0.24856	−0.28616	−0.2112	−0.19375	−0.31439	−0.18672	−0.18157	−0.21136
	Model	−0.12001	−0.09833	−0.16186	−0.3552	−0.12173	−0.31857	−0.27313	−0.06374
	DQM (0)	−0.12001	−0.09833	−0.16186	−0.3552	−0.12173	−0.31857	−0.27313	−0.06374
	DQM (10)	−0.12001	−0.09833	−0.16186	−0.3552	−0.12173	−0.31857	−0.27313	−0.06374
	DQM (100)	−0.12001	−0.09833	−0.16186	−0.3552	−0.12173	−0.31857	−0.27313	−0.06374
	DQM (1,000)	−0.12001	−0.09833	−0.16186	−0.3552	−0.12173	−0.31857	−0.27313	−0.06374
Kurtosis	Observation	2.1911	2.0363	1.7936	1.8217	1.9715	1.9937	1.9781	1.8914
	Model	1.7973	1.8799	1.9203	2.1842	1.9354	2.0148	2.0546	1.9622
	DQM (0)	1.7973	1.8799	1.9203	2.1842	1.9354	2.0148	2.0546	1.9622
	DQM (10)	1.7973	1.8799	1.9203	2.1842	1.9354	2.0148	2.0546	1.9622
	DQM (100)	1.7973	1.8799	1.9203	2.1842	1.9354	2.0148	2.0546	1.9622
	DQM (1,000)	1.7973	1.8799	1.9203	2.1842	1.9354	2.0148	2.0546	1.9622

Note: Descriptive statistics also justify Figure 6. There is a good adjustment of mean and mode towards observation after bias correction, however, skewness and kurtosis are the same as of the model data. This shows that the bell shape of the model is preserved after the bias correction, however, their location changes according to the observational data.

mean characteristics after using DQMs at different numbers, thus highlighting its potential. Similar improved distribution is shown in the case of model statistics as well. Further skewness, which a measure of simple symmetry or no-symmetry of the normal distribution is assessed. In most of the cases, distribution is negatively skewed, except at the stations where mean is negative and positively skewed. After bias correction, the model temperature field distribution, skewness of the distribution at most of the stations reverts towards the skewness of the corresponding observed temperature field. In addition, in most of the cases, negative kurtosis is noticed in the model temperature field, which after bias correction is improved towards the corresponding observed temperature field distribution. Figure 7 shows the box-whisker plot distribution for the model, bias corrected and corresponding observed temperature field at eight stations (Bhakra, Kasol, Suni, Rampur, Kalpa, Namgia, Rakchham and Kaza) in the SRB. The line from lowest to highest temperature values represents the overall data length. The shaded box starts towards the lowest temperature values representing the first quartile while the shaded box ends towards highest temperature value representing the third quartile. The cross line shows the median value of each data set. The figure shows that distributed quantile method has a good capability to correct the model temperature fields. However, the division of data sets into different quantile numbers has a minor difference to bias corrected data sets. However, in all the cases, non-biased model temperature fields are closer to the corresponding observations once bias corrected. There mean as well as their spread is closer to the corresponding observations. Further, these model temperature fields and bias corrected temperature fields with corresponding observed temperature fields are shown in a scatter plot in Figure 8. The figure illustrates the scatter plot of the model temperature field before and after bias correction against the observed temperature at

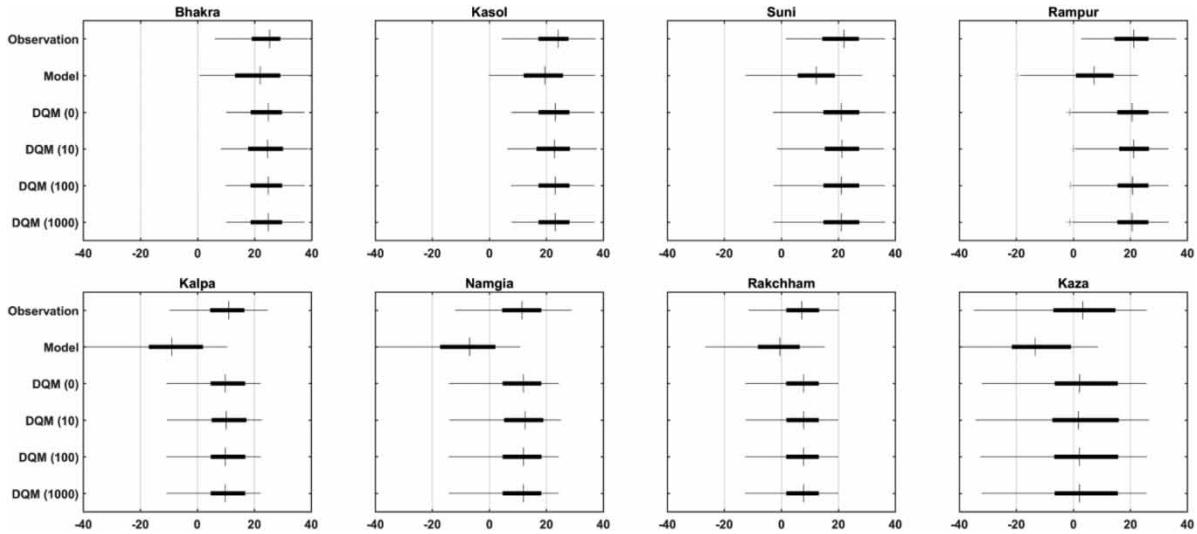

Figure 7 | The box-whisker plot distribution of model temperature field, bias corrected temperature field and corresponding observed temperature field at eight stations (Bhakra, Kasol, Suni, Rampur, Kalpa, Namgia, Rakchham and Kaza) in the SRB. The line from lowest to highest temperature values represents the overall data length. The shaded box starts towards the lowest temperature value and represents the first quartile while the shaded box ends towards the highest temperature value which represents the third quartile. The cross line shows the median value of each data set. DQM stands for distributed quantile mapping and the number within the brackets (0, 10, 100, 1,000) represents the number of quantiles used in the particular study to divide data length.

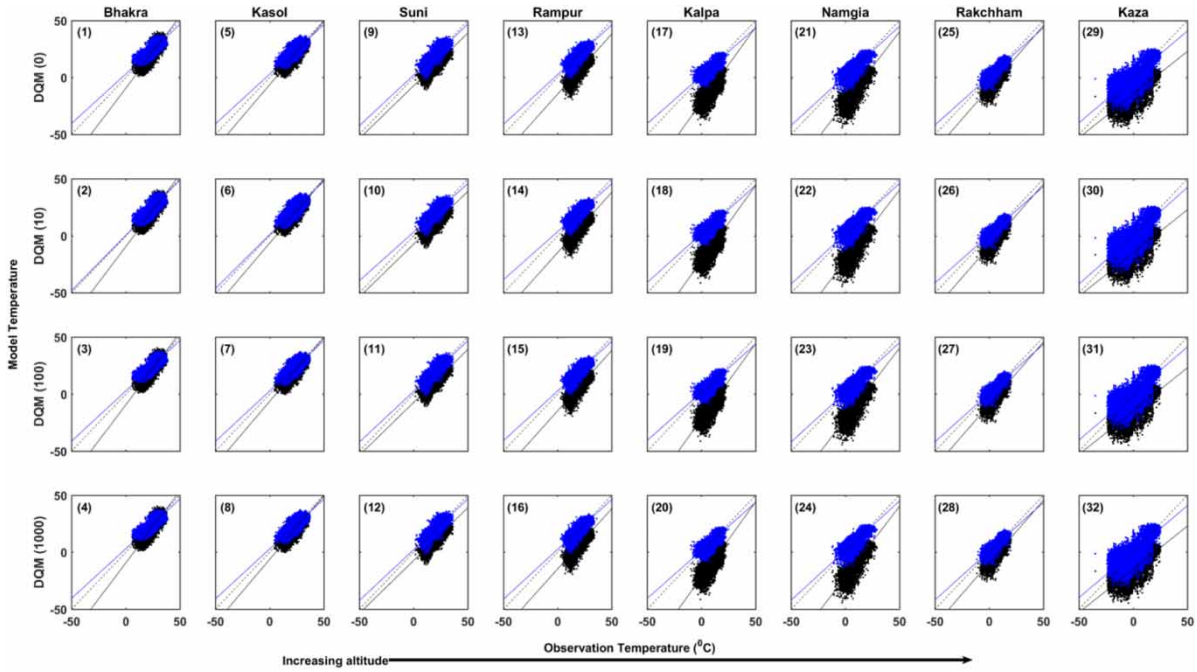

Figure 8 | The scatter plot of the model temperature field before and after bias correction against the observed temperature at eight stations (Bhakra, Kasol, Suni, Rampur, Kalpa, Namgia, Rakchham and Kaza) in the SRB. Black dots represent the uncorrected data sets while dots represent the bias corrected data sets. The CORDEX-REMO is clearly underestimating the temperature as compared to observation which is almost corrected after the bias correction. Black lines represent the regression line between observed and uncorrected data sets while lines represents the regression line between observed and corrected data sets. Black dots represent the $y = x$ line. DQM stands for distributed quantile mapping and the number within the brackets (0, 10, 100, 1,000) represents the number of quantiles used in the particular study to divide data length.

eight stations (Bhakra, Kasol, Suni, Rampur, Kalpa, Namgia, Rakchham and Kaza) in the SRB. The model temperature field underestimates the temperature as compared to the corresponding observed temperature field which is almost corrected after the bias correction. Regression line between observed and uncorrected data sets and the regression line between observed and corrected data sets is shown. Regression lines show distinct improvement upon the bias corrected field at all the eight stations and all improvements are also seen with increased elevations (elevation-dependent changes over the region are not discussed). These DQM methods improve the model data once bias correction is employed.

CONCLUSIONS

Correct estimate of precipitation and temperature field over any river basin is needed to assess hydrological, glaciological and water stress for the downstream habitat and, in addition, to have future assessments based on model inputs as well. In the present work, bias correction demonstration – for precipitation and temperature – is shown over two important river basins of northern India. The proposition of bias correction is to inculcate possible improvement in model fields based on available observation fields, so that model fields after bias correction can be used for other hydrological, glaciological, etc. studies. In addition, bias correction is a pre-requisite for application on model fields for impact studies. By doing so, it removes systematic errors in the model fields which arise either due to initial and boundary forcing provided to RCMs or inherent RCMs limitation of model physics and parameterization schemes.

Therefore, in the present study, bias correction methods are demonstrated over two of the river basins in central Himalayas (UGRB) and western Himalayas (SRB). After employing bias correction, distinct improvements are found in the model fields. It can be seen that precipitation bias correction over the UGRB and temperature bias correction over the SRB of model fields reduces the systematic errors and, thus, will be of extreme guiding help in using these improved data series for future climate impact studies.

ACKNOWLEDGEMENTS

The author acknowledges the Department of Science and Technology (DST), Govt. of India for funding project under National Mission for Sustaining Himalayan Ecosystem (NMSHE) in collaboration with National Institute of Hydrology (NIH), Roorkee, Uttarakhand. Data used in the present study are provided by NIH, Roorkee, Uttarakhand.

DATA AVAILABILITY STATEMENT

The data that support the findings of this study are available from the corresponding author upon reasonable request.

REFERENCES

Akhtar, M., Ahmad, N. & Booji, M. J. 2008 The impact of climate change on the water resources of the Hindukush-Karokorum-Himalaya region under different glacier coverage scenario. *Journal of Hydrology* **355** (1–4), 148–163.

Ali, S., Li, D., Congbin, F. & Khan, F. 2015 Twenty first century climatic and hydrological changes over the Upper Indus Basin of Himalayan region of Pakistan. *Environmental Research Letters* **10**, 1–20.

Bannister, D., Orr, A., Jain, S. K., Holman, I. P., Momblanch, A., Phillips, T., Adeloye, A. J., Snapir, B., Waine, T. W., Hosking, J. S. & Allen-Sader, C. 2019 Bias correction of high resolution regional climate model precipitation output gives the best estimates of precipitation in Himalayan catchments. *Journal of Geophysical Research: Atmospheres* **24**, 14220–14239. doi:10.1029/2019JD030804.

Bharati, L. & Jayakody, P. 2010 *Hydrology of the Upper Ganga River*. International Water Management Institute, Colombo, Sri Lanka, p. 24.

Bookhagen, B. & Burbank, D. W. 2010 Toward a complete Himalayan hydrological budget: spatiotemporal distribution of snowmelt and rainfall and their impact on river discharge. *Journal of Geophysical Research* **115**, F03019. https://doi.org/10.1029/2009JF001426.

Bordoy, R. & Burllando, P. 2013 Bias correction of regional climate model simulations in a region of complex orography. *Journal of Applied Meteorology and Climatology* **52**, 82–101. https://doi.org/10.1175/JAMC-D-11-0149.1.

Choudhary, A. & Dimri, A. P. 2019 On bias correction of summer monsoon precipitation over India from CORDEX-SA simulations. *International Journal of Climatology* **39**, 1388–1403.

Christensen, J. H., Boberg, F., Christensen, O. B. & Lucas-Picher, P. 2008 On the need for bias correction of regional climate change projections of temperature and precipitation. *Geophysical Research Letters* **35** (20). https://doi.org/10.1029/2008GL035694.

Dimri, A. P., Niyogi, D., Barros, A. P., Ridley, J., Mohanty, U. C. & Yasunari, T. 2015 Western disturbances: a review. *Reviews of Geophysics* **53** (2), 225–246.

Dimri, A. P., Yasunari, T., Kotlia, B. S., Mohanty, U. C. & Sikka, D. R. 2016 Indian winter monsoon: present and past. *Earth-science Reviews* **163**, 297–322.

Eriksson, M., Xu, J., Shrestha, A. B., Viaidya, R. A., Nepal, S. & Sanstorm, K. 2009 *The Changing Himalayas: Impact of Climate Change on Water Resources and Livelihood in the Greater Himalayas*. International Centre for Integrated Mountain Development, Kathmandu, Nepal, p. 24.

Li, H., Xu, C.-Y., Beldring, S., Merete, T. L. & Jain, S. K. 2016 Water resources under climate change in Himalayan basins. *Water Resources Management* **30**, 843–859.

Maharana, P. & Dimri, A. P. 2019 The Indian Monsoon: past, present and future. *Proceedings of the Indian National Science Academy* **85** (2), 403–420.

Narula, K. K. & Gosain, A. K. 2013 Modeling hydrology, groundwater recharge and non-point nitrate loadings in the Himalayan upper Yamuna basin. *Science of the Total Environment* **468–469**, S102–S116. https://doi.org/10.1016/j.scitotenv.2013.01.022.

Nepal, S. 2016 Impacts of climate change on the hydrological regime of the Kosi river basin in the Himalayan region. *Journal of Hydro-Environment Research* **10**, 76–89. https://doi.org/10.1016/j.her.2015.12.001.

Norris, J., Carvalho, L. M. V., Jones, C. & Cannon, F. 2015 WRF simulations of two extreme snowfall events associated with contrasting extratropical cyclones over the western and central Himalaya. *Journal of Geophysical Research: Atmospheres* **120**, 3114–3138. https://doi.org/10.1002/2014JD022592.

Norris, J., Carvalho, L. M. V., Jones, C., Cannon, F., Bookhagen, B., Palazzi, E. & Tahir, A. A. 2017 The spatiotemporal variability of precipitation over the Himalaya: evaluation of one-year WRF model simulation. *Climate Dynamics* **49** (5–6), 2179–2204. https://doi.org/10.1007/s00382-016-3414-y.

Palazzi, E., von Hardenberg, J. & Provenzale, A. 2013 Precipitation in the Hindu-Kush Karakorum Himalaya: observations and future scenarios. *Journal of Geophysical Research: Atmospheres* **118**, 85–100. https://doi.org/10.1029/2012JD018697.

Piani, C., Weedon, G. P., Best, M., Gomes, S. M., Viterbo, P., Hagemann, S. & Haerterd, J. O. 2010 Statistical bias correction of global simulated daily precipitation and temperature for the application of hydrological models. *Journal of Hydrology* **395**, 199–215.

Sanjay, J., Krishnan, R., Shrestha, A. B., Rajbhandari, R. & Ren, G.-Y. 2017 Downscaled climate change projection for the Hindu Kush Himalaya region using CORDEX-SA regional climate models. *Advances in Climate Change Research* **8**, 185–198. https://doi.org/10.1016/j.accre.2017.08.003.

Shrestha, M., Acharaya, S. C. & Shrestha, P. K. 2017 Bias correction of climate model for hydrological modeling – are simple methods still useful? *Meteorological Applications* **24**, 531–539. https://doi.org/10.1002/met.1655.

Singh, P. & Kumar, N. 1997 Effect of orography on precipitation in the western Himalayan region. *Journal of Hydrology* **199**, 183–206.

First received 19 May 2020; accepted in revised form 30 June 2020. Available online 5 August 2020